

A simple statistical model describing burnt area through limitations on fire

Bistinas, I², Burton, C^{5, 6}, Kelley, D *¹, Marthews, T¹ and Whitley, R³

¹Centre for Ecology and Hydrology, Maclean Building,
Crowmarsh Gifford, Wallingford, Oxfordshire, United Kingdom

²Vrije Universiteit Amsterdam, Faculty of Earth and Life
Sciences, Amsterdam, Netherlands

³Suncorp Group, Personal Lines Pricing Research, Sydney,
Australia

⁵Met Office UK, Exeter, UK

⁶Geography, University of Exeter, Exeter, UK

November 11, 2016

git info

git url: <https://github.com/douglask3/LimFIRE>

git revision no: 897bca3

Last commit author: douglask3 - Reading, douglas.i.kelley@gmail.com

Branch: (HEAD, doc)

Revision Date: 2016-11-11 12:48:07 +0000

Blue highlights is stuff to decide

pink highlights is yet to be implemented or needs updating.

*Email: douglas.i.kelley@gmail.com Web: douglask3.github.io

Abstract

Aim Spatial and temporal patterns of burnt area are controlled by availability of fuel, fuel moisture, natural and anthropogenic ignitions, and anthropogenic suppression. Here, we map the limitation and sensitivity of burnt area to each of these controls.

Location Global

Methods We describe a simple framework whereby limitations are imposed by: fuel discontinuity; fuel moisture and atmospheric drying potential; lightning and human ignitions; and land use. Limitations are described from remote sensed and meteorological observations and optimized against Global Fire Emissions Database (GFED4s) burnt area observations.

Results Fuel moisture is shown to be the main limitation of fire over much of the world, (44% annual average and 36% during local dry seasons), particularly in the humid forests and cold, slow drying boreal areas. Fuel discontinuity is the next limitation (25% annually and 23% in the dry season), especially in deserts and dry season grasslands. This is followed by land use change (18% annually, 21% dry season) and then ignitions (13% annually, 19% dry season), which is only a significant limiting factor in dry season savanna, where rapid drying of fuel built up during the wet season removes all other natural limitations. In these areas, changes in burnt area are actually more sensitive to other controls, typically land use.

Main conclusions This study contradicts the way basic processes are represented in many global fire models. As ignitions only impact burnt area over a limited geographic extent, better representation of controls imposed by fuel loads and moisture is vital. Human ignitions only contribute to a small increase in global burnt area (2offset by the dramatic impact of suppression through anthropogenic land cover changes. The assumption that humans cause burnt area over much of the world is therefore clearly incorrect, and adequate simulation of suppression through land use should become a priority. This result also has implications when considering ecosystem services of agricultural land and fire management policies

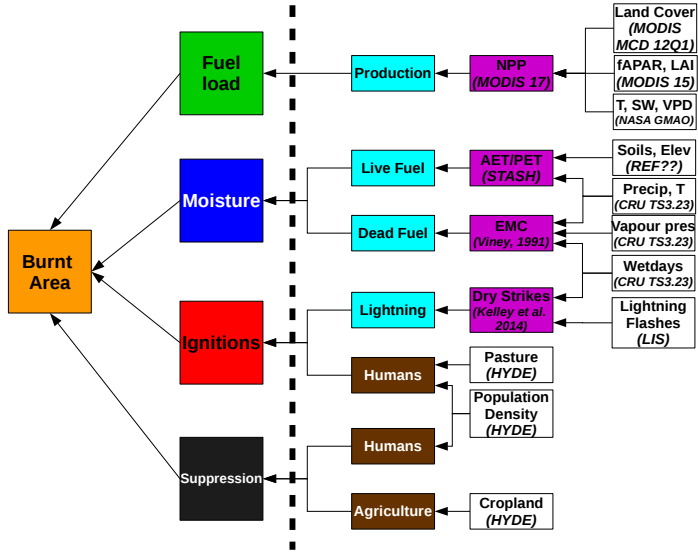


Figure 1: Framework description.

1 Methods

The framework calculates burnt area based on the maximum allowed burnt area from limitations imposed by four controls: fuel, moisture, ignition, and anthropogenic suppression. These controls are described from remote sensed and meteorological observations. Parameters relating controls to fire are optimised against Global Fire Emissions Database (GFED4s) burnt area observations [4]. The framework could probably be used on a range of temporal and spatial resolutions (scale dependency might be something to test in the future?). Here, burnt area is calculated monthly on a 0.5° CRUTS3.22 grid [6], between Jan 2000 and Dec 2010 (the period of data overlap).

1.1 Overview

The framework assumes that 100% burnt area occurs in perfect fire conditions, i.e. complete fuel coverage, no moisture, saturated ignition and no agricultural or urban fragmentation. This is analogous to the dry season in tropical savanna and grasslands [9], particularly parts of Northern Australia

[16] and the Sahel [21] which experience complete burning each year. Burnt area is reduced as each control becomes sub-optimal, i.e. fuel loads become discontinuous (e.g. desert areas) or too moist (e.g. Humid evergreen forests), if there is a lack of ignition (shown to influence interannual variability in parts Southern Australia [2] and probably some other places), or with increased human influence on the landscape (e.g. cropland or urban areas). Fractional burnt area (F) is the product of the maximum allowed burnt area for each control (F_i).

$$F = \prod_i F_i \quad (1)$$

Is it widely known that \prod means product?

A controls maximum burnt area is related to fuel loads, moisture, ignitions or suppression via the logistic function, as per Bistinas et al. [1]:

$$f(x) = 1/(1 + e^{-k \cdot (x - x_0)}) \quad (2)$$

where k described the steepness of the curve and x_0 is the curves midpoint (see figure 2).

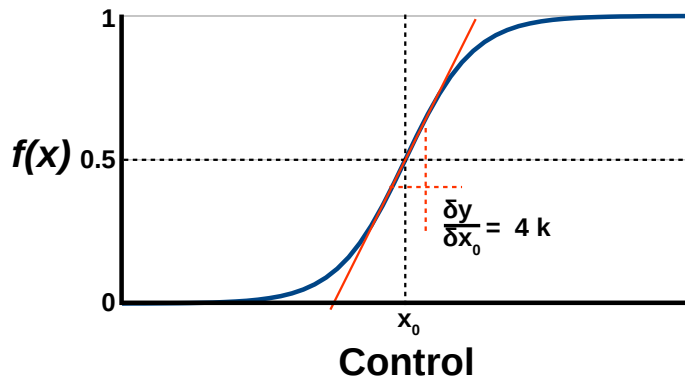


Figure 2: Logistic function.

Fire increases with increasing fuel load (F_w) and ignitions (F_{ig}), and decreases with moisture (F_ω) and anthropogenic suppression (F_s). Therefore:

$$\begin{aligned}
F_w &= f(w) \\
F_\omega &= 1 - f(\omega) \\
F_{ig} &= f(ig) \\
F_s &= 1 - f(s)
\end{aligned} \tag{3}$$

1.2 Inputs

1.2.1 Fuel (w)

The framework will use a measure of fractional cover as a proxy for fuel continuity (i.e. annual mean or maximum fAPAR, as used by Knorr et al. [14, 13] or MODIS fractional cover). Bistinas et al. [1] uses SeaWiFs fAPAR, but this product was discontinued in 2005, so would reduce our comparison period. Other fAPAR/Fractional cover products would probably cover a larger period.

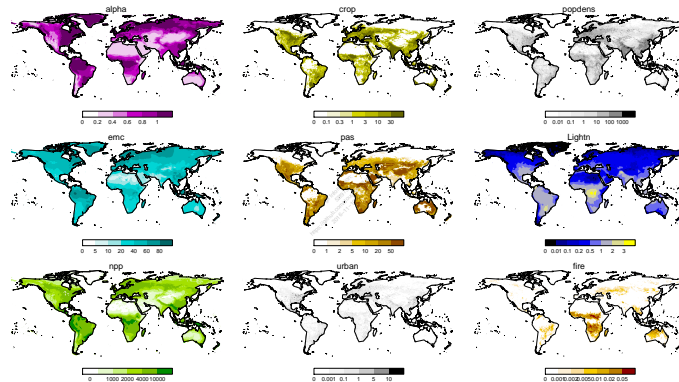


Figure 3: Monthly means of each framework input add units and GFEDv4.

1.2.2 Moisture (ω)

ω represents mean fractional water content of fuel, and combines contributions from soil (i.e from live fuels - α) and atmosphere (atm) coupling:

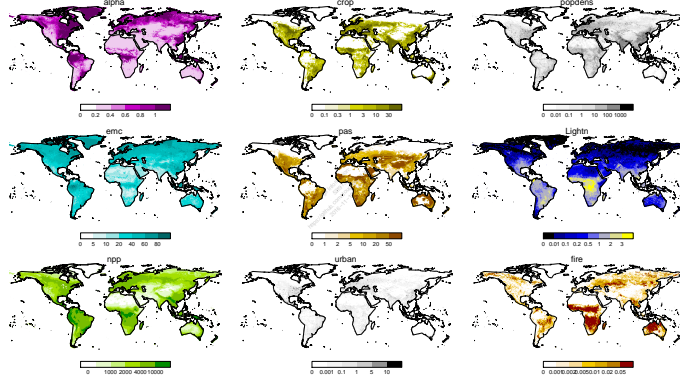


Figure 4: Monthly means during the fire season for each input `add_units` and GFEDv4 training data. “Fire season” is defined as the month with heighest burnt area, calculated each year.

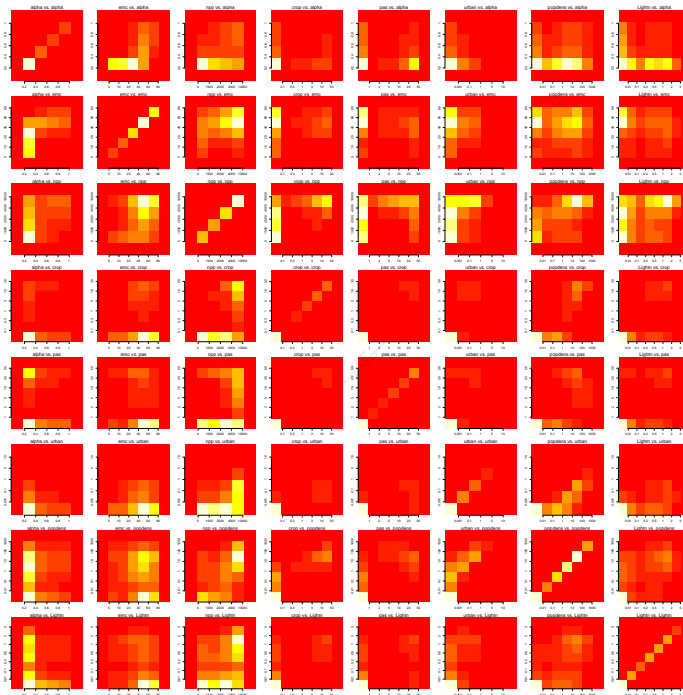


Figure 5: Input correlations.

$$\omega = (\alpha + M \cdot atm) / (1 + M) \quad (4)$$

where M is an optimised parameter, representing the relative importance of atmospheric to soil coupling.

Soil-coupled contribution. The ratio of actual to potential evaporation [α 17], a measure of available soil water in relation to plant demand, is used to describe fractional water content soil-coupled fuels as per Harrison et al. [7], Bistinas et al. [1]. α is calculated from CRUTS3.22 monthly mean temperature, cloud cover and precipitation using the STASH model [20] r-package [24]. At the moment, elevation, is set to zero and field capacity to 140 - Rhys, I guess this will have to change? Any suggestions for data?. STASH was spun up by recycling 1950 climate data for 40 years and then run from 1950 to 2010. Simulated α from 2000-2010 used for the rest of the analysis.

Atmosphere-controlled (atm) could be represented using either STASH outputs or by a simple equilibrium moisture content calculation (m_{mq}).

- **STASH.** The ratio of condensation rate (Con) and atmospheric evaporative demand (i.e PET) could be used to calculate “fuel drying speed” (FDS):

$$FDS = \frac{Con}{PET} \quad (5)$$

here, when $FDS > 1$, daily condensation occurs more rapidly than drying, and fuel load moisture will increase, and when $FDS < 1$, fuel dries faster than condensation and fuel moisture will decrease.

There are a few things to consider here:

1. How should precip be included? Options are to add it to the Con term:

$$FDS = \frac{Con + Pr}{PET} \quad (6)$$

or give FDS a maximum value of 1, which is also equivalent to a wetday:

$$FDS = WD + (1 - WD) \cdot \min(1, Con/PET) \quad (7)$$

where WD is fractional wet days

or something else

2. Is PET being double counted (I couldn't quite get my head round this bit). If so, there could be a way of combining soil and atmosphere:

$$\omega_* = \frac{AET + C_n}{PET} \quad (8)$$

or maybe

$$\omega_* = \frac{AET}{PET - C_n} \quad (9)$$

which could also be combined with rainfall:

$$\omega = WD + (1 - WD) \cdot \min(1, \omega_*) \quad (10)$$

- m_{mq} is currently used and is calculated from [22] which combines daily precipitation (Pr) and atmospheric drying potential via temperature (T) and relative humidity (H_r):

$$m_{mq,daily} = \begin{cases} 10 - (T - H_r)/4, & \text{if } Pr \leq 3\text{mm} \\ 100, & \text{otherwise} \end{cases} \quad (11)$$

On a monthly timestep, this simplifies to:

$$m_{mq} = (10 - (T - H_r)/4) \cdot (1 - WD) + 100 \cdot WD \quad (12)$$

where WD is the monthly fraction of wet days from CRU TS3.22, where a wetday is defined as a day where $Pr > 3\text{mm}$. H_r was calculated as the ratio of actual to saturated vapour pressure ref??:

$$H_r = 100 \cdot AVP/SVP \quad (13)$$

monthly AVP is from CRUTS.22. SVP was calculated from mean monthly temperature as per Walter et al. [23]

$$SVP = 6.11 \cdot 10^{\frac{7.5 \cdot T}{237.5 + T}} \quad (14)$$

1.2.3 Ignitions (ig)

Ignition combines sources from lightning (L_{ig}), pasture and the local population.

$$ig = L_{ig} + P \cdot Pasture + D \cdot Population Density \quad (15)$$

where P and D are optimized parameters.

We could also add background ignitions:

$$ig = 1 + N \cdot L_{ig} + P \cdot Pasture + D \cdot Population Density \quad (16)$$

where N , P and D are opimized paramters describing the contribution of their respective ignition source relative to background ignitions.

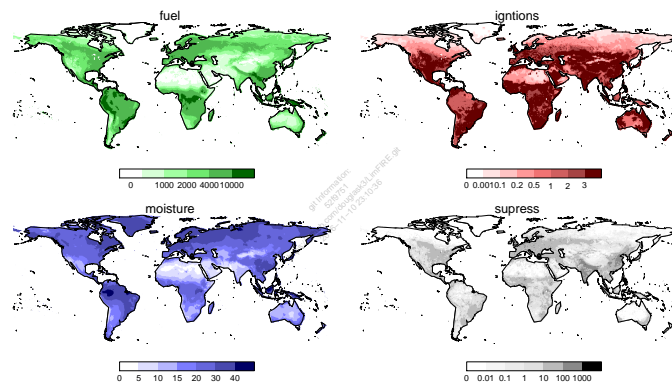


Figure 6: Monthly means of each control. add units?

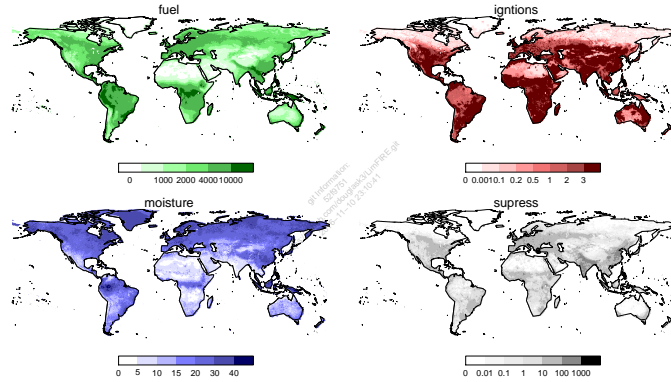


Figure 7: Monthly means of each control during the fire season. add units?

Lightning is calculated from the Lightning Imaging Sensor flash count climatology (LIS [3], <http://grip.nsstc.nasa.gov/>). Are there other products that could be used instead? This product contains both cloud-to-ground (*CG* - available for ignition) and inter-cloud (not available for ignitions) strikes. *CG* lighting is calculated using Kelley et al. [11]:

$$L_{ig} = FL * \min(1, 0.0408 \cdot FL^{-0.4180}) \quad (17)$$

where *FL* is the flash count recorded by LIS over a 0.5 degree cell.

Pasture and population density are taken from the HYDE dataset [12], and are interpolated from a decadal to a monthly timestep.

1.2.4 Supression (*s*)

Suppression combines urban and cropland area and population density

$$s = \text{urban} + C \cdot \text{Crop} + H \cdot \text{Population Density} \quad (18)$$

where *C* and *H* are optimised parameters.

Urban and cropland areas are taken from HYDE and processed as per pasture and population desnity (section 1.2.3)

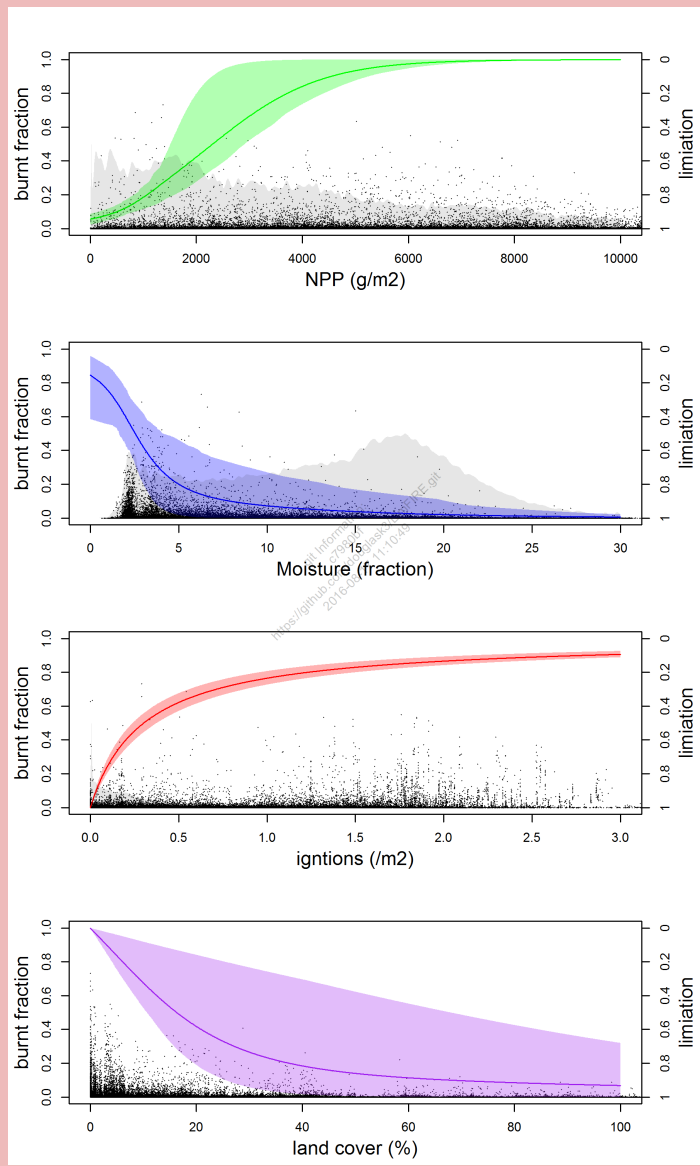


Figure 8: Limitation contribution for each control.

1.3 Optimization

The framework is optimised against GFED4s observations [4] using normalised least squares in R [18]. This is likely to change, though, so I won't describe it anymore for the moment. GFED4s was re-gridded from 0.25 to a 0.5° resolution using "resample" in the raster r-package [8].

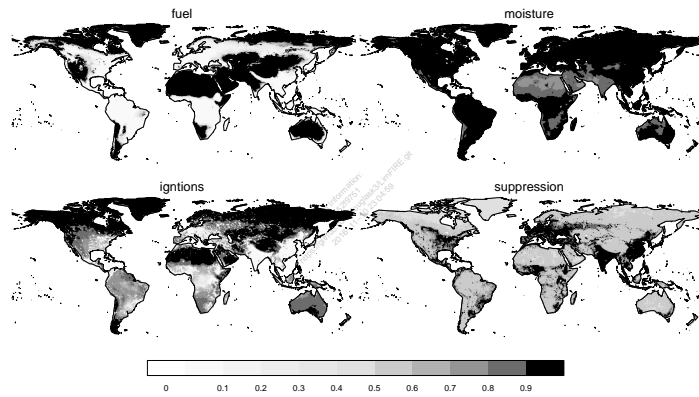


Figure 9: Annual average limitation of each control.

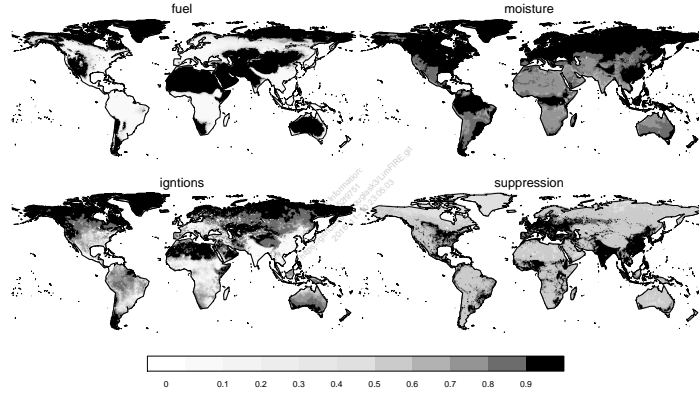


Figure 10: Fire season average limitation of each control.

Optimization is performed on equation 1 to 3, 4, 15, 16 and 18 (figure 8). Each control optimizes two parameters associated with its maximum expected burnt area (equations 2 and 3, see figure 2). Parameters relating

Table 1: Optimized parameters obviously, to be filled in.

Parameter	Bound	Value
Fuel	k_w	
	$x_{0,w}$	
Moisture	k_ω	
	$x_{0,\omega}$	
	M	
Ignitions	k_{ig}	
	$x_{0,ig}$	
	P	
Human Suppression	D	
	k_s	
	$x_{0,s}$	
	C	
	H	

different fuel moisture, ignition and suppression sources are also optimized (see table 1)

1.4 Benchmarking

To assess performance of reconstructed burnt area, we'll probably use NME to compare reconstructed fire from the framework with GFED (figure 11) for annual average, seasonal and inter-annual comparisons [10] as recommended by fireMIP Rabin et al. [19], Hantson et al. [5], and maybe McFaddens R^2 as per [1]. Annual average NME comparison comes out at 0.46, which is better than benchmarking null models described in Kelley et al. [10], and outperforms coupled vegetation-fire models contributing to fireMIP [5], although this is to be expected as the framework is driven by, and optimised to, observations [10].

1.5 Analysis

1.5.1 Limitation

The relative importance of each controls was assessed as:

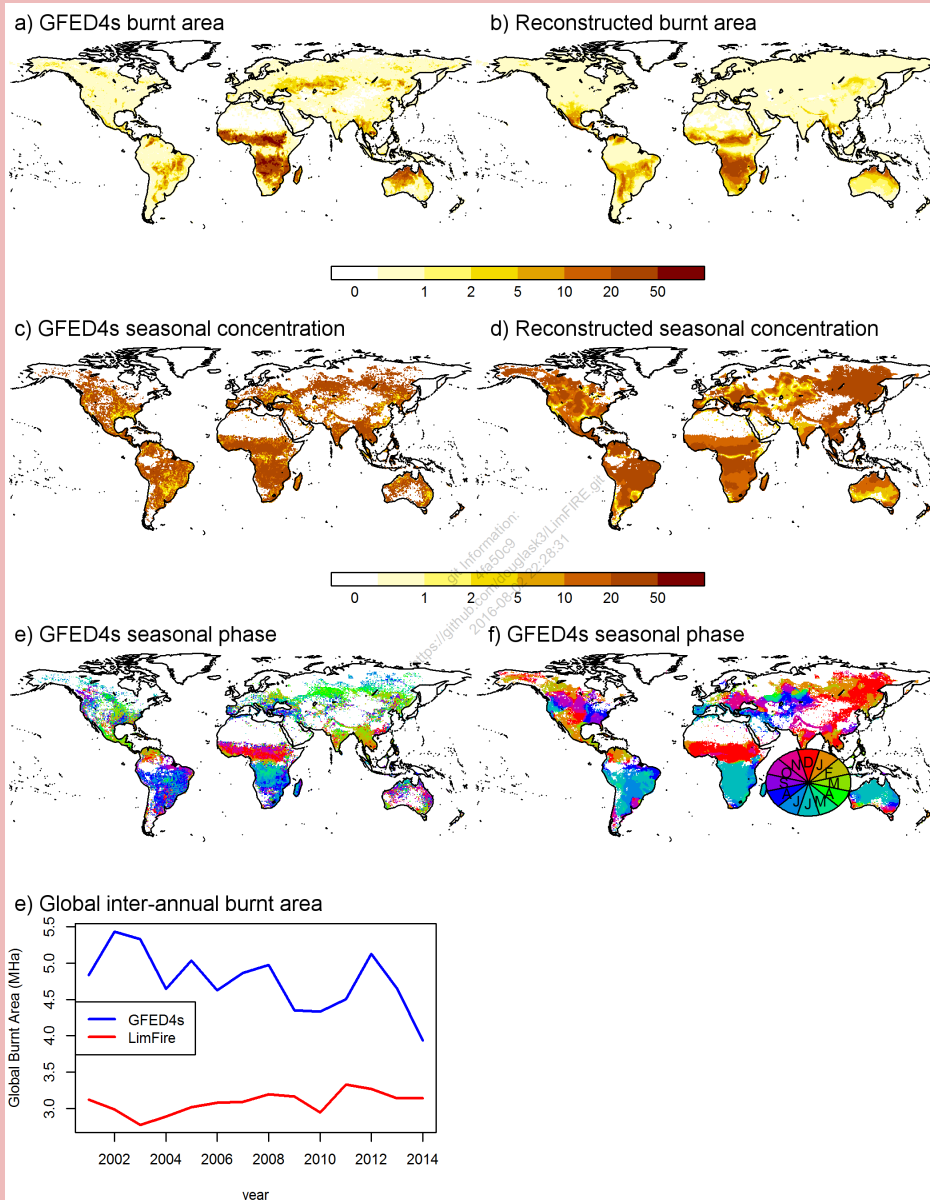


Figure 11: Benchmark comparisons against GFED4s [4].

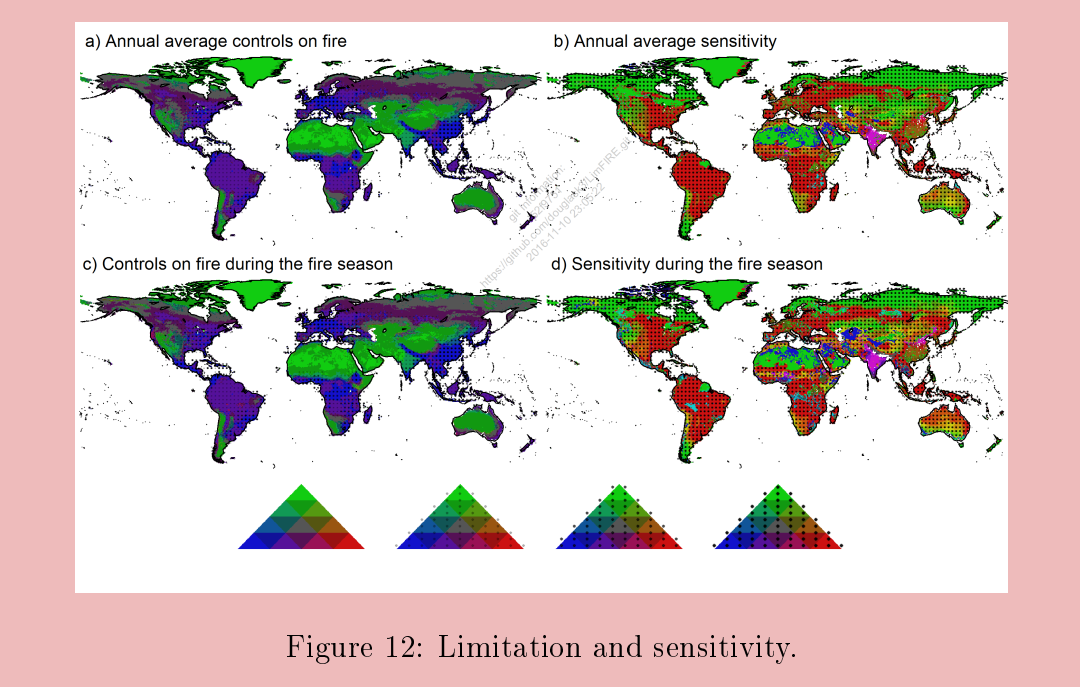


Figure 12: Limitation and sensitivity.

$$L_{i,X}^- = \frac{L_{i,X}}{\sum_j L_{j,X}} \quad (19)$$

where $L_{i,X} = 1 - F_{i,X}$ is the individual contribution of each control i for conditions X . By definition, $\sum_i L_{i,X}^- = 1$, for each location (figures 12 and 13).

1.5.2 Sensitivity

There are two ways I can think of that we could assess sensitivity to each control. We could compare the gradient of each control around the cells current conditions (figure 12). Alternatively, we could calculate the required change in each control to induce a “significant” change in fire regime. The first would be a nice way of classifying different locations, along the same lines as limitations (i.e, Australian Tropical Savanna is xx % sensitive to changes in fuel load, and yy % to moisture - see e.g. figure 12). The second

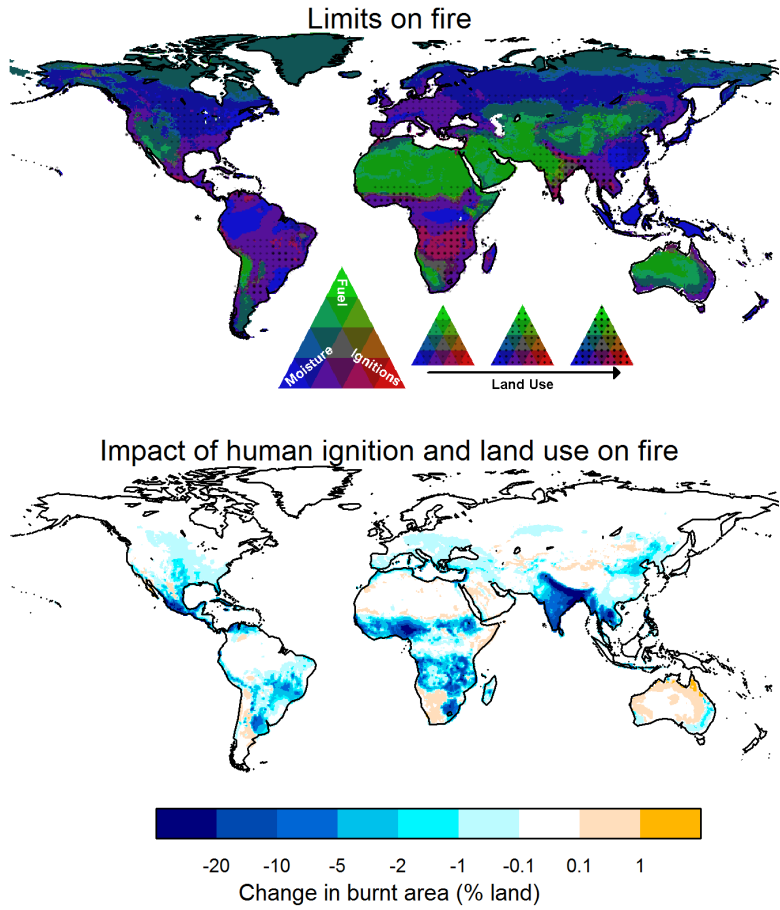


Figure 13: AGU plot.

would be harder to normalise across controls, but might be easier to relate to actual changes in climate (i.e. xx ° increase in temperature would increase fire to expected levels for Savanna - see e.g. figure 14; increase in yy % of agricultural land would reduce fire in non-agricultural land to that expected for forests etc)

options 1

$$\partial \bar{L}_{i,x} = \frac{\partial L_{i,x} \cdot \Pi_j L_{j,x}}{L_{i,x}} \quad (20)$$

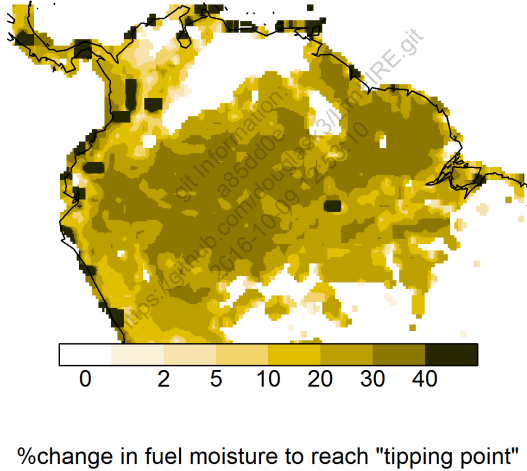


Figure 14: Required change in % fuel moisture content to induce savanna-level fire in the Amazon.

where $\partial L_{i,x}$ is the gradient of $L_{i,x}$ relative to the maximum possible gradient of L_i , occurring when $x = x_0$ i.e:

$$\partial l_{i,x} = \frac{\partial l_{i,x}/\partial X}{\partial l_{i,x_0}/\partial x} \quad (21)$$

options 2 for measuring sensitivity is to calculate the change required for a control to alter burnt area enough to induce major alterations in i.e vegetation cover. For example, assessing amazon risk of fire-induced tipping point. Holding the contribution of ignition, fuel load and land use constant, we could calculate the change in moisture needed to increase burnt area to the level expected for Savanna (roughly 1% in South America according to [15]). It would be easy to work out a required change in climate variables (humidity, temperature, ET etc, or any combination of these) required to hit

this 'fire tipping point' (figure 14).

2 Some other results

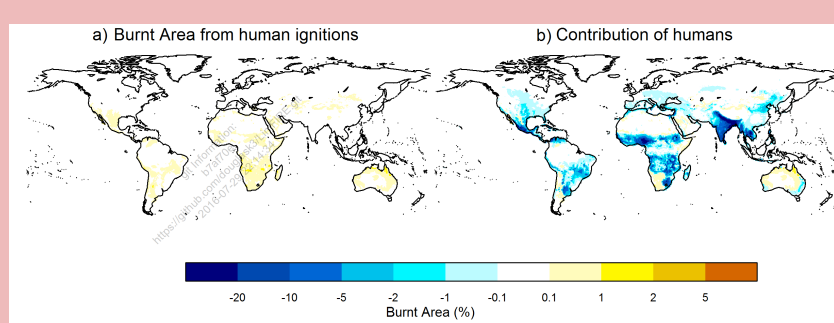


Figure 15: Human impact on burnt area. a) Increases in burnt area from human induced fire starts. b) Changes in burnt area from human fire starts and suppression.

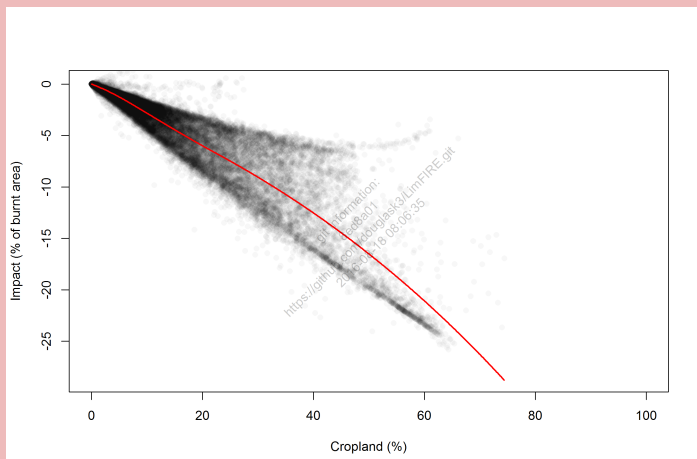


Figure 16: The impact of cropland on burnt area in non-cropland within the same grid cell.

References

- [1] I Bistinas, SP Harrison, IC Prentice, JM Pereira, et al. Causal relationships versus emergent patterns in the global controls of fire frequency. 2014.
- [2] Ross A Bradstock. A biogeographic model of fire regimes in australia: current and future implications. *Global Ecology and Biogeography*, 19(2):145–158, 2010.
- [3] H Christian, R Blakeslee, S Goodman, D Mach, M Stewart, D Buechler, W Koshak, J Hall, William Boeck, K Driscoll, et al. The lightning imaging sensor. In *NASA conference publication*, pages 746–749. NASA, 1999.
- [4] Louis Giglio, James T. Randerson, and Guido R. van der Werf. Analysis of daily, monthly, and annual burned area using the fourth-generation global fire emissions database (gfed4). *Journal of Geophysical Research: Biogeosciences*, 118(1):317–328, 2013. ISSN 2169-8961. doi: 10.1002/jgrg.20042. URL <http://dx.doi.org/10.1002/jgrg.20042>.

- [5] Stijn Hantson, Almut Arneth, Sandy P Harrison, Douglas I Kelley, I Colin Prentice, Sam S Rabin, Sally Archibald, Florent Mouillet, Steve R Arnold, Paulo Artaxo, et al. The status and challenge of global fire modelling. *Biogeosciences*, 13(11):3359–3375, 2016.
- [6] I Harris, PD Jones, TJ Osborn, and DH Lister. Cru ts3. 22: Climatic research unit (cru) time-series (ts) version 3.22 of high resolution gridded data of month-by-month variation in climate (jan. 1901–dec. 2013). ncas british atmospheric data centre. *NCAS British Atmospheric Data Centre*, 24, 2014.
- [7] Sandy P Harrison, Jennifer R Marlon, and Patrick J Bartlein. Fire in the earth system. In *Changing climates, earth systems and society*, pages 21–48. Springer, 2010.
- [8] Robert J. Hijmans. *raster: Geographic Data Analysis and Modeling*, 2016. URL <http://CRAN.R-project.org/package=raster>. R package version 2.5-8.
- [9] D I Kelley. *Modelling Australia Fire Regimes*. PhD thesis, Macquarie University, 2014.
- [10] DI Kelley, I Colin Prentice, SP Harrison, H Wang, M Simard, JB Fisher, and KO Willis. A comprehensive benchmarking system for evaluating global vegetation models. *Biogeosciences*, 10:3313–3340, 2013.
- [11] DI Kelley, SP Harrison, IC Prentice, et al. Improved simulation of fire-vegetation interactions in the land surface processes and exchanges dynamic global vegetation model (lpx-mv1). 2014.
- [12] Kees Klein Goldewijk, Gerard Van Drecht, and AF Bouwman. Mapping contemporary global cropland and grassland distributions on a 5×5 minute resolution. *Journal of Land Use Science*, 2(3):167–190, 2007.
- [13] W Knorr, L Jiang, and A Arneth. Climate, co 2 and human population impacts on global wildfire emissions. *Biogeosciences*, 13(1):267, 2016.
- [14] Wolfgang Knorr, Thomas Kaminski, Almut Arneth, and Ulrich Weber. Impact of human population density on fire frequency at the global scale. *Biogeosciences*, 11(4):1085–1102, 2014.

- [15] Caroline ER Lehmann, Sally A Archibald, William A Hoffmann, and William J Bond. Deciphering the distribution of the savanna biome. *New Phytologist*, 191(1):197–209, 2011.
- [16] Brett P Murphy, Ross A Bradstock, Matthias M Boer, John Carter, Geoffrey J Cary, Mark A Cochrane, Roderick J Fensham, Jeremy Russell-Smith, Grant J Williamson, and David MJS Bowman. Fire regimes of australia: a pyrogeographic model system. *Journal of Biogeography*, 40(6):1048–1058, 2013.
- [17] I Colin Prentice, Martin T Sykes, and Wolfgang Cramer. A simulation model for the transient effects of climate change on forest landscapes. *Ecological modelling*, 65(1):51–70, 1993.
- [18] R Core Team. *R: A Language and Environment for Statistical Computing*. R Foundation for Statistical Computing, Vienna, Austria, 2015. URL <https://www.R-project.org/>.
- [19] S. S. Rabin, J. R. Melton, G. Lasslop, D. Bachelet, M. Forrest, S. Hantson, F. Li, S. Mangeon, C. Yue, V. K. Arora, T. Hickler, S. Kloster, W. Knorr, L. Nieradzik, A. Spessa, G. A. Folberth, T. Sheehan, A. Voulgarakis, I. C. Prentice, S. Sitch, J. O. Kaplan, S. Harrison, and A. Arneth. The fire modeling intercomparison project (firemip), phase 1: Experimental and analytical protocols. *Geoscientific Model Development Discussions*, 2016:1–31, 2016. doi: 10.5194/gmd-2016-237. URL <http://www.geosci-model-dev-discuss.net/gmd-2016-237/>.
- [20] Martin T Sykes, I Colin Prentice, and Wolfgang Cramer. A bioclimatic model for the potential distributions of north european tree species under present and future climates. *Journal of Biogeography*, pages 203–233, 1996.
- [21] Guido R Van Der Werf, James T Randerson, Louis Giglio, Nadine Gobron, and AJ Dolman. Climate controls on the variability of fires in the tropics and subtropics. *Global Biogeochemical Cycles*, 22(3), 2008.
- [22] Neil R Viney. A review of fine fuel moisture modelling. *International Journal of Wildland Fire*, 1(4):215–234, 1991.
- [23] Ivan A Walter, Richard G Allen, Ronald Elliott, ME Jensen, D Itenfisu, B Mecham, TA Howell, R Snyder, P Brown, S Echings, et al. Asce’s

standardized reference evapotranspiration equation. In *Proc. of the Watershed Management 2000 Conference, June*, 2000.

- [24] Rhys Whitley, Colin Prentice, Wang Han, and Douglas Kelley. *rstash: STASH R-Package*, 2014. URL <http://github.com/rhyswhitley/rstash>. R package version 2.0.